Chen J, Li Y, Chopp M (2000) Intracerebral transplantation of bone marrow with BDNF after MCAO in rat. *Neuropharmacology* 39:711–6

Chen JL, Li Y, Wang L, Zhang ZG, Lu DY, Lu M *et al* (2001) Therapeutic benefit of intravenous administration of bone marrow stromal cells after cerebral ischemia in rats. *Stroke* 32:1005–11

Chen X, Katakowski M, Li Y, Lu D, Wang L, Zhang L *et al* (2002*a*) Human bone marrow stromal cell cultures conditioned by traumatic brain tissue extracts: growth factor production. *J Neurosci Res* 69:687–91

Chen X, Li Y, Wang L, Katakowski M, Zhang L, Chen J *et al* (2002*b*) Ischemic rat brain extracts induce human marrow stromal cell growth factor production. *Neuropathology* 22:275–9

Chopp M, Li Y (2002) Treatment of neural injury with marrow stromal cells. *Lancet Neurol* 1:92–100

Chopp M, Zhang XH, Li Y, Wang L, Chen J, Lu D *et al* (2000) Spinal cord injury in rat: treatment with bone marrow stromal cell transplantation. *Neuroreport* 11:3001–5

Coffin RS, Thomas SK, Thomas DP, Latchman DS (1998) The herpes simplex virus 2 kb latency associated transcript (LAT) leader sequence allows efficient expression of downstream proteins which is enhanced in neuronal cells: possible function of LAT ORFs. *J Virol* 79:3019–26

Conget PA, Minguell JJ (2000) Adenoviral-mediated gene transfer into *ex vivo* expanded human bone marrow mesenchymal progenitor cells. *Exp Hematol* 28:382–90

Damme AV, Driessche TV, Collen D, Chuah MKL (2002) Bone marrow stromal cells as targets for gene therapy. *Curr Gene Ther* 2:195–209

David AR, Thomas AK (2002) Using bone marrow stromal cells for treatment of stroke. *Neurology* 59:486–7

Dormady SP, Bashayan O, Dougherty R, Zhang XM, Basch RS (2001) Immortalized multipotential mesenchymal cells and the hematopoietic microenvironment. *J Hematother Stem Cell Res* 10:125–40

Friedenstein AJ, Ivanov-Smolenski AA, Chajlakjan RK, Gorskays UF, Kuralesova AI, Latzinik NW *et al* (1978) Origin of bone marrow stromal mechanocytes in radiochimeras and heterotopic transplants. *Exp Hematol* 6:440–4

Hayashi K, Morishita R, Nakagami H, Yoshimura S, Hara A, Matsumoto K *et al* (2001) Gene therapy for preventing neuronal death using hepatocyte growth factor: *in vivo* gene transfer of HGF to subarachnoid space prevents delayed neuronal death in gerbil hippocampal CA1 neurons. *Gene Therapy* 8:1167–73

Haynesworth SE, Baber MA, Caplan AI (1996) Cytokine expression by human marrow-derived mesenchymal progenitor cells *in vitro*: effects of dexamethasone and IL-1 alpha. *J Cell Physiol* 166:585–92

Jin H, Yang R, Li W, Ogasawara AK, Schwall R, Eberhard DA *et al* (2003) Early treatment with hepatocyte growth factor improves cardiac function in experimental heart failure induced by myocardial infarction. *J Pharmacol Exp Ther* 304:654–60

Kim BJ, Seo JH, Bubien JK, Oh YS (2002) Differentiation of adult bone marrow stem cells into neuroprogenitor cells *in vitro*. *Neuroreport* 13:1185–8

Kurozumi K, Nakamura K, Tamiya T, Kawano Y, Ishii K, Kobune M *et al* (2005) Mesenchymal stem cells that produce neurotrophic factors reduce ischemic damage in the rat middle cerebral artery occlusion model. *Mol Ther* 11:96–104

Kurozumi K, Nakamura K, Tamiya T, Kawano Y, Kobune M, Hirai S *et al* (2004) BDNF gene-modified mesenchymal stem cells promote functional recovery and reduce infarct size in the rat middle cerebral artery occlusion model. *Mol Ther* 9:189–97

Li Y, Chen J, Chen XG, Wang L, Gautam SC, Xu YX *et al* (2002) Human marrow stromal cell therapy for stroke in rat: neurotrophins and functional recovery. *Neurology* 59:514–23

Li Y, Chen J, Wang L, Lu M, Chopp M (2001) Treatment of stoke in rat with intracarotid administration of marrow stromal cells. *Neurology* 56:1666–72

Li Y, Chopp M, Chen J, Wang L, Gautam SC, Xu YX *et al* (2000) Intrastriatal transplantation of bone marrow nonhematopoietic cells improves functional recovery after stroke in adult mice. *J Cerebr Blood Flow Metab* 20:1311–9

Lilley CE, Groutsi F, Han Z, Palmer JA, Anderson PN, Latchman DS *et al* (2001) Multiple immediate-early gene-deficient herpes simplex virus vectors allowing efficient gene delivery to neurons in culture and widespread gene delivery to the central nervous system *in vivo*. *J Virol* 75:4343–56

Longa EZ, Weinstein PR, Carlson S, Cummins R (1988) Reversible middle cerebral artery occlusion without craniectomy in rats. *Stroke* 20:84–91

Matsumoto K, Nakamura T (1996) Emerging multipotent aspects of hepatocyte growth factor. *J Biochem (Tokyo)* 119:591–600

Matsumoto K, Nakamura T (1997) Hepatocyte growth factor (HGF) as a tissue organizer for organogenesis and regeneration. *Biochem Biophys Res Commun* 239: 639–44

McIntosh K, Bartholomew A (2000) Stromal cell modulation of the immune system. *Graft* 3:324–8

Miyazawa T, Matsumoto K, Ohmichi H, Katoh H, Yamashima T, Nakamura T (1998) Protection of hippocampal neurons from ischemia-induced delayed neuronal death by hepatocyte growth factor: a novel neurotrophic factor. *J Cereb Blood Flow Metab* 18:345–8

Nakamura T, Nawa K, Ichihara A (1984) Partial purification and characterization of hepatocyte growth factor from serum of hepatectomized rats. *Biochem Biophys Res Commun* 122:1450–9

Nakano K, Migita M, Mochizuki H, Shimada T (2001) Differentiation of transplanted bone marrow cells in the adult mouse brain. *Transplantation* 71:1735–40

Pages JC, Bru T (2004) Toolbox for retrovectorologists. *J Gene Med* 6(Suppl 1):S67–82

Palmer JA, Branston RH, Lilley CE, Robinson MJ, Groutsi F, Smith J *et al* (2000) Development and optimization of herpes simplex virus vectors for multiple long-term gene delivery to the peripheral nervous system. *J Virol* 74:5604–18

Paxinos G, Watson C, Pennisi M, Topple A (1985) Bregma, lambda and the interaural midpoint in stereotaxic surgery with rats of different sex, strain and weight. *J Neurosci Methods* 13:139–43

Phinney DG (2002) Building a consensus regarding the nature and origin of mesenchymal stem cells. *J Cell Biochem* 38:7–12

Raymond AS, Matthew TM, George TW, Robert AS, Charisse D, Frank RS (1990) A semiautomated method for measuring brain infarct volume. *J Cerebr Blood Flow Metab* 10:290–3

Rempe DA, Kent TA (2002) Using bone marrow stromal cells for treatment of stroke. *Neurology* 59:486–7

Schallert T, Kozlowski DA, Humm JL, Cocke RR (1997) Use-dependent structural events in recovery of function. *Adv Neurol* 73:229–38

Shimamura M, Sato N, Oshima K, Aoki M, Kurinami H, Waguri S *et al* (2004) Novel therapeutic strategy to treat brain ischemia: overexpression of hepatocyte growth factor gene reduced ischemic injury without cerebral edema in rat model. *J Circ* 109:424–31

Sun W, Funakoshi H, Nakamura T (2002*a*) Localization and functional role of hepatocyte growth factor (HGF) and its receptor c-met in the rat developing cerebral cortex. *Mol Brain Res* 103:36–48

Sun W, Funakoshi H, Nakamura T (2002*b*) Overexpression of HGF retards disease progression and prolongs life span in a transgenic mouse model of ALS. *J Neurosci* 22:6537–48

Trono D (2000) Lentiviral vectors: turning a deadly foe into a therapeutic agent. *Gene Therapy* 7:20–3

Tsuzuki N, Miyazawa T, Matsumoto K, Nakamura T, Shima K, Chigasaki H (2000) Hepatocyte growth factor reduces infarct volume after transient focal cerebral ischemia in rats. *Acta Neurochir Suppl* 76:311–6

Watanabe T, Okuda Y, Nonoguchi N, Zhao MZ, Kajimoto Y, Furutama D *et al* (2004) Post-ischemic intraventricular administration of FGF-2 expressing adenoviral vectors improves outcome and reduces infarct volume after transient focal cerebral ischemia in rats. *J Cerebr Blood Flow Metab* 24:1205–13

Williams LR, Varon S, Peterson GM, Wictorin K, Fischer W, Bjorklund A *et al* (1986) Continuous infusion of nerve growth factor prevents basal forebrain neuronal death after fimbria fornix transaction. *Proc Natl Acad Sci USA* 83:9231–5

Woodbury D, Schwarz EJ, Prockop DJ, Black IB (2000) Adult rat and human bone marrow stromal cells differentiate into neurons. *J Neurosci Res* 61:364–70

Histol Histopathol (2006) 21: 729-742

http://www.hh.um.es

Histology and Histopathology

Cellular and Molecular Biology

Histological recovery of the hepatocytes is based on the redox system upregulation in the animal models of mutant superoxide dismutase (SOD)1-linked amyotrophic lateral sclerosis

M. Kato[1], S. Kato[2], Y. Abe[3], T. Nishino[3], E. Ohama[2], M. Aoki[4] and Y. Itoyama[4]

[1]Division of Pathology, Tottori University Hospital, [2]Department of Neuropathology, Institute of Neurological Sciences, Faculty of Medicine, Tottori University, Yonago, Japan, [3]Department of Biochemistry and Molecular Biology, Nippon Medical School, Tokyo and [4]Department of Neuroscience, Division of Neurology, Tohoku University Graduate School of Medicine, Sendai, Japan

Summary. Histological rescue of superoxide dismutase1 (SOD1)-mutated hepatocytes from mutant SOD1 stress is investigated from the viewpoint of upregulation of the redox system [peroxiredoxin (Prx) and glutathione peroxidase (GPx)]. Histopathological and immunohistochemical studies using antibodies against PrxI/PrxII/GPxI were carried out on specimens from four different strains of animal models of mutant SOD1-linked familial amyotrophic lateral sclerosis (ALS). In the livers of the ALS animal models in the presymptomatic stage without motor neuron loss, both swollen and eosinophilic hepatocytes with vacuolation pathology were observed. After developing motor deficits, this swelling and vacuolation ceased to be apparent. In the terminal stage when severe motor neuron loss was observed, these hepatocytes recovered and appeared normal. In redox system-related immunohistochemical preparations, almost all of the normal hepatocytes expressed the redox system-related enzymes PrxI/PrxII/GPxI. In the presymptomatic stage, some hepatocytes did not express redox system-related enzymes. After clinical onset, over 75% of hepatocytes showed overexpression of PrxI/PrxII/GPxI, i. e., upregulation of the redox system. At the end stage, near normal PrxI/PrxII/GPxI expression was observed again in the hepatocytes. Redox system upregulation in SOD1-mutated hepatocytes rescues hepatocytes from the mutant SOD1 stress that leads to motor neuron death.

Offprint requests to: Masako Kato, M.D., Ph.D., Division of Pathology, Tottori University Hospital, Nishi-cho 36-1, Yonago 683-8504, Japan. e-mail: makato@grape.med.tottori-u.ac.jp, Shinsuke Kato, M.D., Ph.D., Department of Neuropathology, Institute of Neurological Sciences, Faculty of Medicine, Tottori University, Nishi-cho 36-1, Yonago 683-8504, Japan. e-mail: kato@grape.med.tottori-u.ac.jp

Key words: Amyotrophic lateral sclerosis, Hepatocyte, Redox system, Peroxiredoxin, Superoxide dismutase1

Introduction

In general, living cells under aerobic conditions produce reactive oxygen species (ROSs) during physiological processes and in response to external stimuli such as ultraviolet radiation and chemical agents. In order to protect themselves from potentially destructive ROSs, cells have developed antioxidant enzyme defense systems. In these systems, there are two groups of enzymes; the enzymes of the first group convert superoxide radicals to hydrogen peroxide (H_2O_2), and the enzymes of the second group convert H_2O_2 to harmless water (H_2O) and oxygen (O_2). In the first group, three isoforms of superoxide dismutase (SOD) [EC 1.15.1.1] have been identified: SOD1, SOD2, and SOD3 (Fridovich, 1986; Abe and Okazaki, 1987), and in the second group, there are the peroxiredoxin-(Prx-) and glutathione peroxidase-(GPx-) families, as well as catalase that is localized in peroxisomes. The enzymes of the Prx- and GPx-families are considered to be important players that directly control the redox system.

The Prx-families have been identified in a large number of organisms (Chae et al., 1993, 1994; Prosperi et al., 1993; Hirotsu et al., 1999b; Hofmann et al., 2002). PeroxiredoxinI (PrxI) is an intracellular antioxidant protein that is expressed preferentially in the liver (Iwahara et al., 1995). PeroxiredoxinII (PrxII) is also a novel organ-specific antioxidative enzyme that is expressed in the mammalian central nervous system (Matsumoto et al., 1999; Kato et al., 2004) as well as the liver. The GPx-family is composed of at least four GPx

isoforms in mammals (de Haan et al., 1998), and GPxI is thought to be the major enzyme responsible for removing intracytoplasmic H_2O_2. Furthermore, the redox system regulates various control mechanisms in signal transduction and gene expression (Sen and Packer, 1996). This redox signal transduction is linked to important biological systems such as apoptosis, cellular differentiation, immune response and growth control (Jin et al., 1997; Wen and Van etten, 1997).

Amyotrophic lateral sclerosis (ALS) is a fatal neurodegenerative disorder that selectively involves both upper and lower motor neurons (Kato et al., 2003). The prevalence rate of ALS is approximately 5 to 10 cases per 100,000 population (de Belleroche et al., 1996). Five to ten per cent of ALS cases are familial, although most ALS cases are sporadic (Hudson, 1981; Juneja et al., 1997). The disease has been studied for over 130 years since Charcot and Joffroy (1869) first reported it in 1869. In 1991, linkage analysis of certain familial ALS (FALS) patients demonstrated that the genetic locus is strongly linked to chromosome 21q (Siddique et al., 1991). Deng et al. (1993) and Rosen et al. (1993) indicated in 1993 that this locus partially overlaps the genetic locus of SOD1 on chromosome 21. Based on this discovery, human mutated SOD1-expressing transgenic mice have been developed and human mutated-SOD1 causes progressive motor neuron degeneration and death with a similar course to that in human ALS (Gurney et al., 1994). Nagai et al. have successfully produced two types of transgenic rat expressing human SOD1 with H46R and G93A mutations (Nagai et al., 2001). Pathologically, mutant SOD1 causes motor neuron death in the in vivo milieu where it exists, that is, in familial ALS patients with SOD1 gene mutation and transgenic animals expressing human mutant SOD1 (Kato et al., 2003). The exact mechanism of the motor neuron death based on mutant SOD1 is still unclear although there are many hypotheses, including copper toxicity, hydroxy radical toxicity, peroxynitrite toxicity, and aggregation toxicity (Kato et al., 1999, 2000, 2003). In addition, ALS is a heterogeneous disease including sporadic ALS of unknown etiology, familial ALS with SOD1 gene mutation and transgenic animal models with human mutant SOD1. Despite the heterogeneous pathogenesis of ALS, its essential neuropathology is motor neuron death. In the spinal cord, the common, consistent neuropathological finding among sporadic ALS of unknown etiology, familial ALS with SOD1 gene mutation and transgenic animal models with human mutant SOD1 is loss of the anterior horn cells (Kato et al., 1999, 2000, 2003). Because SOD1 is most abundant in the liver (Westman and Marklund, 1981; Iwahara et al., 1995), and mutant SOD1 is concentrated in the liver milieu where mutant SOD1 exists, the toxicity of mutant SOD1 should be most evident in the liver. Anterior horn cells of the spinal cord and hepatocytes are equally involved in mutant SOD1 stress. However, the essential pathological feature of SOD1-mutated FALS patients and human mutant SOD1-linked ALS model animals is cell death in anterior horn cells but not in hepatocytes. In other words, although anterior horn cells and hepatocytes are under the same mutant SOD1 stress, cell death is observed histopathologically only in the anterior horn cells. Given that the redox system-related proteins PrxI, PrxII and GPxI (PrxI/PrxII/GPxI) that are directly linked to SOD1 (mutant SOD1) are also most abundant in hepatocytes (Westman and Marklund., 1981; Iwahara et al., 1995), we sought to elucidate immunohistochemically the mechanism by which SOD1-mutated hepatocytes survive while SOD1-mutated anterior horn cells die.

Materials and methods

Animal models

Histochemical and immunohistochemical studies were carried out on specimens from ALS animal models: transgenic mice and rats carrying the overexpressed human mutant SOD1 genes. The G93A mice used in this study were two types of transgenic mice carrying the overexpressed human G93A mutant SOD1 gene: high copy G93A mice (G1H, B6SJL-TgN[SOD1-G93A]1Gur; 20-30 copies of the transgene) (G1H-G93A mice) and low copy G93A mice (G1L, B6SJL-TgN[SOD1-G93A]1Gur^{dl};12-16 copies of the transgene) (G1L-G93A mice)(Jackson Laboratory, Bar Harbor, ME, USA). The amount of human SOD1 in RBC lysates of G1H-G93A mice was 3.4 times higher than the G1L-G93A mice (Gurney et al., 1994). The G93A rat was a transgenic line (G93A-39) in which the level of human SOD1 with the G93A mutation was 2.5 times the level of endogenous rat SOD1 (Nagai et al., 2001). The H46R rat used in this study was a transgenic line (H46R-4) in which the level of human SOD1 with the H46R mutation was 6 times the level of endogenous rat SOD1 (Nagai et al., 2001).

The G1H-G93A mice were examined the liver and the spinal cord specimens at 90 (n=2), 100 (n=2), 110 (n=3) and 120 (n=3) days of age. The G1L-G93A mice were examined at 90 (n=1), 100 (n=1), 120 (n=1), 150 (n=1), 180 (n=1), 190 (n=1), 215 (n=1), 230 (n=1) and over 250 (n=2) days of age. As mouse controls, we also examined the liver and the spinal cord specimens of each of ten age-matched littermates of the G1H-G93A and G1L-G93A mice. The G93A rats were examined at 70 (n=1), 90 (n=1), 110 (n=1), 130 (n=1), 150 (n=1) and over 180 (n=3) days after birth. The H46R rats were sacrificed for spinal cords at 110 (n=1), 135 (n=1), 160 (n=1), 170 (n=2) and over 180 (n=3) days after birth and were examined for livers at over 180 days after birth. The detailed clinical signs and pathological characteristics of the H46R and G93A rats have been demonstrated previously (Nagai et al., 2001). As rat controls, we investigated the spinal cord specimens of each of eight age-matched littermates of H46R and G93A rats. Mice and rats were anesthetized with sodium pentobarbital (0.1 ml/100g body weight). After perfusion

of the animals via the aorta with physiological saline at 37°C, they were fixed by perfusion with 4% paraformaldehyde in 0.1 M cacodylate buffer (pH 7.3). The livers and the spinal cords were removed and then postfixed in the same solution. This study was approved by the Institutional Animal Care and Use Committee of Tottori University (Permission No. 03-S-18).

Autopsy specimens

Histochemical and immunohistochemical studies were performed on archival, buffered 10% formalin-fixed, paraffin-embedded liver and spinal cord tissues obtained at autopsy from one long-term surviving FALS patient with a clinical course of 11 years. The clinicopathological characteristics of the FALS patient were reported previously (Kato et al., 1996, 1997). SOD1 analysis revealed FALS patient had a two-base-pair deletion at codon 126 (frame-shift 126 mutation) (Kato et al., 1996). As human controls, we examined autopsy specimens of the pathologically normal livers and spinal cord from 5 neurologically and neuropathologically normal individuals (3 male, 2 females; aged 45-68 years).

Histochemistry and immunohistochemistry

After fixation, the specimens were embedded in paraffin, cut into 4-μm-thick or 6-μm-thick sections and examined by light microscopy. Liver sections were stained by hematoxylin and eosin (HE), and spinal cord sections were stained by the following histochemical methods: HE, Klüver-Barrera, Holzer and Bielschowsky stains. Rat PrxI was over-expressed using the *Escherichia coli* strain BL21 (DE3) cells harboring the expression plasmid pET3c (Novagen, Darmstadt, Germany)-PrxI and purified by the methods described previously (Hirotsu et al., 1999a). Rat PrxII, which contained a 6-His-tagged sequence at the amino-terminal region, was over-expressed using the *Escherichia coli* strain BL21 (DE3) cells harboring the expression plasmid pET30a (Novagen, Darmstadt, Germany)-PrxII. The His-tagged PrxII was purified by a Ni^{2+}-nitrilotriacetate column (Qiagen GmhH, Hilden, Germany) and then digested with enterokinase. Finally, the purified PrxII was passed through an Erapture Agarose column for removal of enterokinase (Novagen). The PrxI /PrxII genes were prepared from a rat liver cDNA library (Takara Biomedicals, Otsu, Japan) by PCR using the primers 5'- AGCCATATGTCTTC AGGAAATGCAA -3', forward and 5- TCGGATCC TCACTTCTGCT TAGAGAAA TACTC-3', reverse for PrxI, as well as the primers 5'-TTCCATGGCCTCCG GCAACGCGCACAT-3', forward and the primers 5'-TTGGATCCATCTCAGTTGTGTTTGGAG-3', reverse for PrxII, respectively. NdeI/BamHI and NcoI/BamHI sites were underlined. Utilizing these purified recombinant rat PrxI (amino acids 1–199) and PrxII (amino acids 1–198), the rabbit polyclonal antibodies against the recombinant rat PrxI/PrxII were prepared by the modified method of Kato et al. (2004).

Representative paraffin sections were used for immunohistochemical assays. The following primary antibodies were used: a newly-produced rabbit polyclonal antibody against rat PrxI [diluted 1:2000 in 1% bovine serum albumin-containing phosphate-buffered saline (BSA-PBS), pH 7.4], a newly-produced rabbit polyclonal antibody against rat PrxII [diluted 1: 2,000 in 1% BSA-PBS, pH 7.4], an affinity–purified rabbit antibody against a synthetic peptide corresponding to the carboxyl terminal region of PrxII (amino acids 184-198: NH2-KPNVDDSKEYFSKHN-COOH. These amino acid sequences are homologous with those of each carboxyl terminal region of the human, rat or mouse PrxII.) (concentration: 1 μg/ml) (Kato et al., 2004), a polyclonal antibody to GPxI [diluted 1: 2,000 in 1% BSA-PBS, pH 7.4] (Kato et al., 2004).

Anti-PrxI antibody was applied to liver sections and anti-PrxII antibody was applied to spinal cord and liver sections because PrxI was contained in the liver but was not contained in the neuron and PrxII was localized in both the neuron and the liver. Sections were deparaffinized, and endogenous peroxidase activity was quenched by incubation for 30 min with 0.3% H_2O_2. The sections were then washed in PBS. Normal serum homologous with the secondary antibody was used as a blocking reagent. Tissue sections were incubated with the primary antibodies for 18 h at 4°C. PBS-exposed sections served as controls. With respect to the preabsorption test, some sections were incubated with anti-PrxI or anti-PrxII polyclonal antibody that had been preabsorbed with an excess amount of the PrxI or PrxII peptide, respectively. Bound antibodies were visualized by the avidin-biotin-immunoperoxidase complex (ABC) method using the appropriate Vectastain ABC Kit (Vector Laboratories, Burlingame, CA, USA) and 3,3'-diaminobenzidine tetrahydrochloride (DAB; Dako, Glostrup, Denmark) as chromogen.

Western blot analysis

This analysis was carried out on 20 fresh specimens from the livers of G1H-G93A mice at 4 different points after birth: 90 days of age (n=2), 100 days of age (n=2), 110 days of age (n=3), and 120 days (n=3). Specimens of livers from control littermate mice were also taken at 4 different points after birth: 90 days of age (n=2), 100 days of age (n=2), 110 days of age (n=3), and 120 days (n=3). In brief, specimens were homogenized in Laemmli sample buffer (Bio-Rad, Hercules, CA, USA) containing 2% sodium dodecyl sulfate (SDS), 25% glycerol, 10% 2-mercaptoethanol, 0.01% bromophenol blue, and 62.5 mM Tris-HCl (pH 6.8). The samples were heated at 100°C for 5 min. Exact 20-μg amounts of soluble protein extracts from the samples were separated on SDS-polyacrylamide gels (4%-20% gradient, Bio-Rad) and transferred by electroblotting to Immobilon PVDF (Milipore, Bedford, MA, USA). After blocking

with 5% nonfat milk for 30 min at room temperature, the blots were incubated overnight at 4°C with the antibody against PrxI. Binding to PrxI was visualized with the Vectastain ABC Kit and DAB. Appropriate molecular weight markers (Bio-Rad) were included in each run.

Results

Clinical course and histopathology

G1H-G93A transgenic mice

The time of clinical onset in the G1H-G93A mice was approximately 100 days after birth. The number of anterior horn cells in the spinal cord of the G1H-G93A mice examined at 90 days after birth was not significantly lower than that of the age-matched littermates, whereas neuropil vacuolation was observed. The anterior horn cells in the G1H-G93A mice at 100 days of age were slightly less abundant and contained many vacuoles and a few Lewy body-like hyaline inclusions (LBHIs). The G1H-G93A mice examined at 110 and 120 days of age revealed severe loss of the anterior horn cells, and also showed many inclusions and neuropil vacuoles, i. e., they had inclusion- and vacuolation-pathologies. The spinal cords of the littermate mice did not show any distinct histopathological findings.

In the presymptomatic stage of the first 90 days after birth, two kinds of cells- swollen hydropic hepatocytes and eosinophilic hepatocytes-were found (Fig. 2A). The swollen hepatocytes had clear nuclei and a bright half-translucent cytoplasm that contained a few vacuoles about 5 μm in diameter. The eosinophilic hepatocytes had condensed nuclei and a dark eosinophilic cytoplasm with some vacuoles about 2 μm in diameter. The population of swollen hepatocytes was about 70% of total hepatocytes and the eosinophilic cells accounted for the remainder (Table 1). The eosinophilic hepatocytes were scattered and intermingled among the swollen hepatocytes. Some intersinusoidal cells also contained vacuoles about 1 μm in diameter. Although both kinds of hepatocytes were still observed at 100 days of age, the small sized-eosinophilic hepatocytes represented about 80% of the cell population and the proportion of swollen hepatocytes was correspondingly lower (Fig. 2B). Fewer

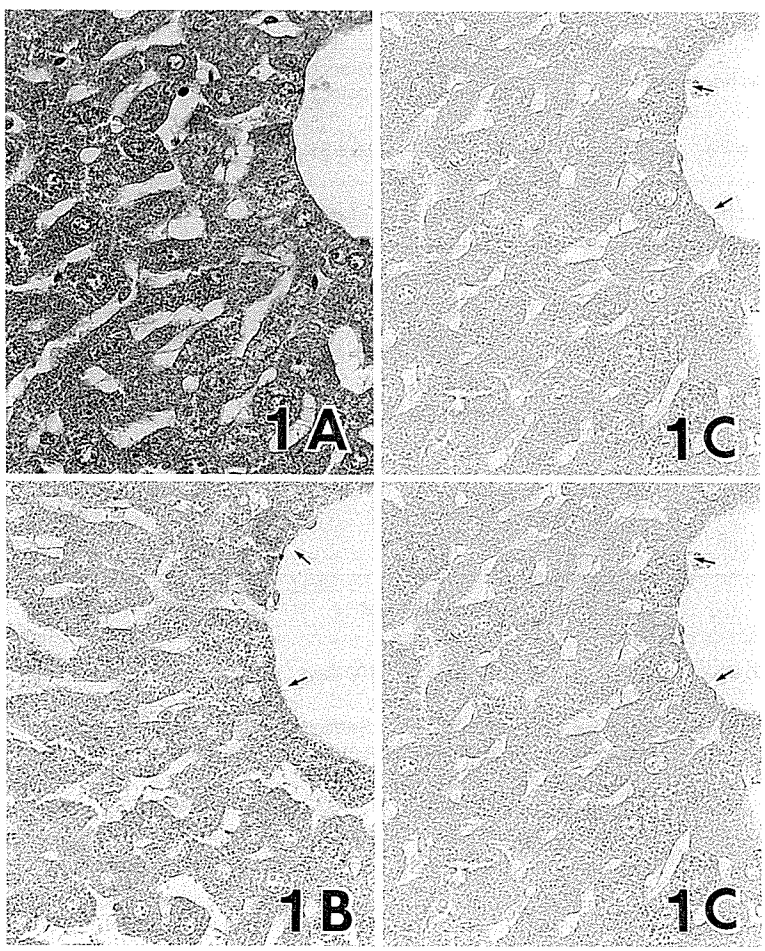

Fig. 1. Hematoxylin and eosin (HE) staining **(A)**, and immunohistochemical staining of the liver sections in control littermate mice for Peroxiredoxinl (Prxl) **(B)**, PeroxiredoxinII (PrxII) **(C)** and Glutathione peroxidasel (GPxl) **(D)**. **A.** The livers of the littermate mice do not show any distinct histopathological findings. **B-D.** Prxl, PrxII and GPxl are expressed in the cytoplasm of almost all hepatocytes. Hepatocytes in the periportal areas stain more strongly for Prxl/PrxII/GPxl than those in the periterminal vein areas (arrows). x 230

vacuoles were present in the cytoplasm of the swollen hepatocytes, although the size of the vacuoles was unchanged. The vacuoles of the eosinophilic hepatocytes became smaller than those of the eosinophilic hepatocytes at 90 days of age, (~1 μm in diameter). Most intersinusoidal cells had shrunken cytoplasm with small (~1 μm) vacuoles. At 110 days of age, almost all of the hepatocytes were normal in HE preparations; neither swollen hydropic hepatocytes nor eosinophilic hepatocytes were observed. No vacuoles were observed in the hepatocytes or intersinusoidal cells. The histological findings in the liver at 120 days of age, corresponding to the end stage (Fig. 2C), were almost the same as those of the control G1H-G93A littermate mice. The intersinusoidal cells also appeared normal in HE preparations. In contrast to the anterior horn cells in the spinal cord, intracytoplasmic eosinophilic inclusions like LBHIs were not observed in the hepatocytes throughout the disease course. The livers of the G1H-G93A littermate mice did not show any distinct histopathological findings (Fig. 1A). Dramatic histopathological changes in the G1H-G93A mouse hepatocytes were observed during the disease course from the presymptomatic stage to the onset (Table 1), in marked contrast to the situation in the spinal cord.

G93A and H46R transgenic rats

The clinical courses and neuropathological findings in G93A and H46R transgenic rats have been reported by Nagai et al. (2001). As expected, the G93A rats showed clinical motor signs at around 125 days of age, and the G46R rats developed motor deficits at approximately 145 days of age. When we focused on the anterior horn cells of the spinal cords of G93A rats, the numbers of anterior horn cells at 70, 90 and 110 days of

Table 1. Histopathological characteristics in the livers of G1H-G93A and G1L-G93A mice and G93A rats during the course of the disease.

G1H-G93A mice	Presymptomatic stage				The onset		Motor deficit stage	End stage
Days after birth	90 days				100 days		110 days	120 days
HE staining	Swollen hepatocytes		Eosinophilic hepatocytes		Swollen hepatocytes	Eosinophilic hepatocytes	Normal hepatocytes	Normal hepatocytes
Percentage*	76 ± 2%		24 ± 2%		17 ± 3%	83 ± 3%	100%	100%
Size of vacuoles	5 μm		2 μm		5 μm	1 μm	-	-
G93A rat	**Presymptomatic stage**				**The onset**		**Motor deficit stage**	**End stage**
Days after birth	70 days	90 days	110 days		130 days		150 days	Over 180 days
HE staining	Normal hepatocytes	Normal hepatocytes	Swollen hepatocytes	Eosinophilic hepatocytes	Normal hepatocytes	Small-sized hepatocytes		Small-sized hepatocytes	Normal hepatocytes
Percentage*	100%	100%	83 ± 1%	3%	14 ± 1%	100%		100%	100%
Size of vacuoles	-	2 μm	3 μm	1 μm	-	1 μm		1 μm	-
G1L-G93A mice	**Presymptomatic stage**				**The onset**		**Motor deficit stage**	**End stage**
Days after birth	110 days	120 days	150 days		180 days	190 days	215 days	Over 250 days
HE staining	Normal hepatocytes	Normal hepatocytes	Swollen hepatocytes	Normal hepatocytes	Swollen hepatocytes	Swollen hepatocytes	Small-sized hepatocytes	Normal hepatocytes
Percentage*	100%	100%	73 ± 5%	27 ± 5%	100%	100%	100%	100%
Size of vacuoles	1~2 μm	2 μm	5 μm	2 μm	5 μm	5 μm	2 μm	-

Percentage* means the percentage of each hepatocyte number to total cell number.

age were almost the same as for the age-matched littermates of G93A rats, although the G93A rats at 90 and 110 days of age showed vacuolation-pathology including neuropil vacuoles. At 70 days of age, no distinct histological changes were found in the livers of the G93A rats. At 90 days of age, a few vacuoles of about 2 μm in diameter began to appear in the cytoplasm of the normal appearing hepatocytes (Table 1). The intersinusoidal cells appeared almost normal. At 110 days of age, in the preclinical stage, swollen hydropic

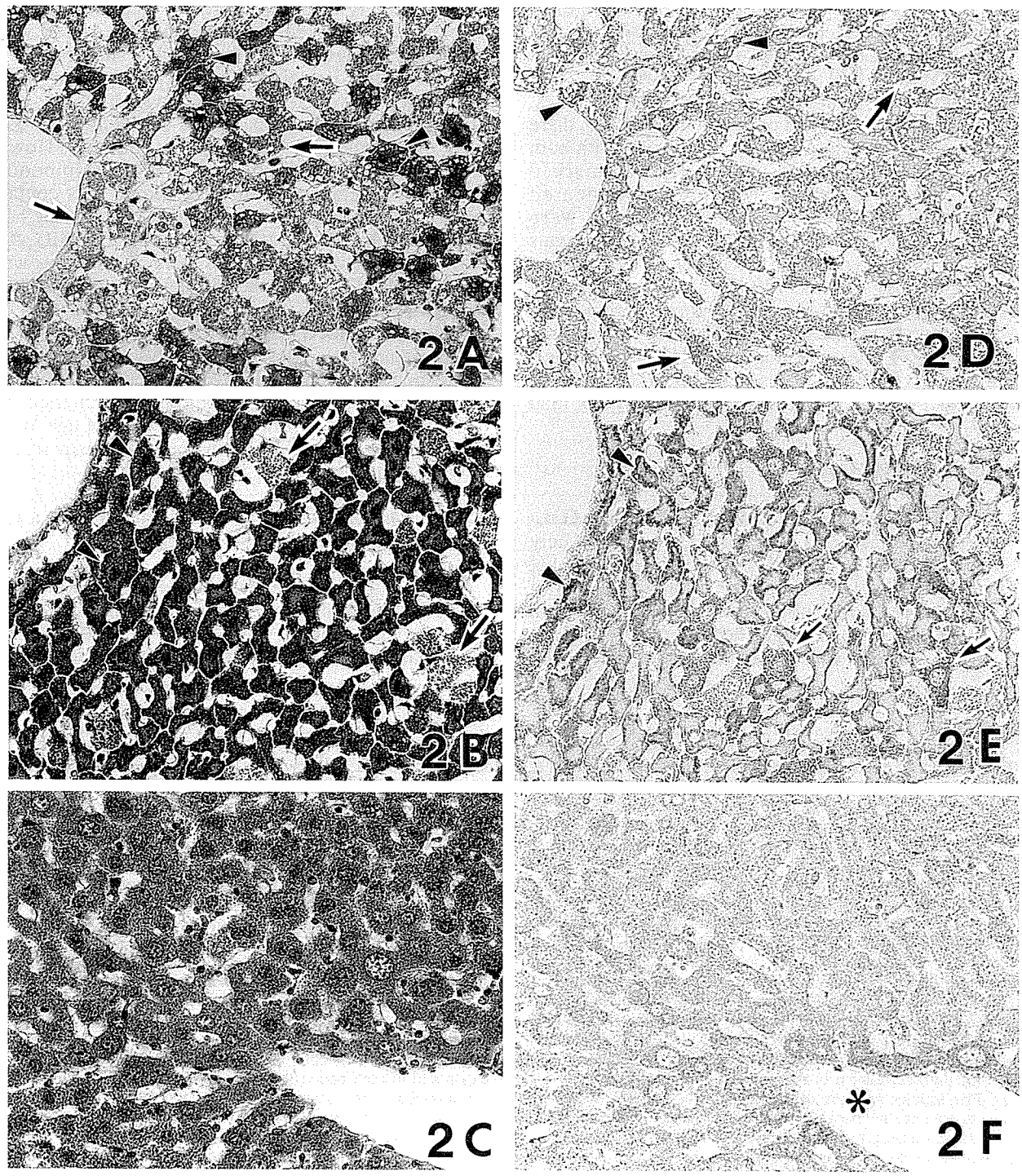

hepatocytes and dark eosinophilic hepatocytes were observed in addition to normal hepatocytes. These two types of hepatocytes in G93A rats were histologically identical to those in HE preparations from G1H-G93A mice. The proportions of each type of hepatocytes were: swollen hydropic hepatocytes, approximately 83%,; eosinophilic hepatocytes, about 3%,; normal hepatocytes, about 14%. The swollen hepatocytes contained some vacuoles about 3 μm in diameter. The eosinophilic hepatocytes shrunken and the dense eosinophilic cytoplasm contained vacuoles about 1μm in diameter. However, the normal appearing hepatocytes at 110 days of age did not contain vacuoles. The intersinusoidal cells contained small (~1 μm) vacuoles. In G93A rats at 130, 150 and over 180 days of age, there was a loss of anterior horn cells in association with both inclusion- and vacuolation-pathologies. In marked contrast, almost all of the hepatocytes appeared histologically normal in HE preparations and were smaller than those of the littermates. Some hepatocytes at 130 days of age contained vacuoles about 1 μm in diameter (Fig. 3A). Beyond 180 days of age, the period corresponding to the end stage when there were marked losses of anterior horn cells, most hepatocytes of both G93A and H46R rats were normal in HE preparations, although a few small vacuoles were observed in some hepatocytes (Table 1). The intersinusoidal cells also appeared almost normal.

G1L-G93A transgenic mice

As expected, the time of clinical onset in the G1L-G93A mice from Jackson Laboratory was approximately 185 days after birth. In the G1L-G93A mice examined at 90, 100, 120, 150 and 180 days after birth, the number of anterior horn cells was not significantly changed in contrast with that of the age-matched littermates of G1L-G93A mice, although the G1L-G93A mice at 90, 100, 120, 150 and 180 days of age showed vacuolation-pathology and the G1L-G93A mouse at 180 days of age showed a few inclusions. In G1L-G93A mice at 190, 215, 230 and over 250 days of age, there were significant losses of anterior horn cells, and both inclusion- and vacuolation-pathologies were present.

At the preclinical stage of 110 and 120 days of age, vacuoles about 2 μm in diameter were already present in the cytoplasm of the hepatocytes in the G1L-G93A mice, although the structures of hepatic lobules and hepatocytes appeared normal (Table 1). At 150,180 and 190 days of age, many hepatocytes showed hydropic change: approximately 60% of hepatocytes at 150 days of age were swollen hepatocytes with hydropic change, and almost all of the hepatocytes at 180 and 190 days of age were hydropic hepatocytes (Table 1). However, eosinophilic hepatocytes were not conspicuous. In addition, several irregular cytoplasmic slits containing some fluid-like material were outstanding in the hepatic cytoplasm at 180 and 190 days of age (Fig. 3B). At 215 days of age, small hepatocytes were observed, as was the case for the G93A rats at 150 days of age. In addition, there were small vacuoles about 2 μm that were distributed in the periphery of the cytoplasm of these small hepatocytes. Beyond 250 days of age, the period corresponding to the end stage, the hepatocytes appeared almost normal in HE preparations. The intersinusoidal cells were almost normal after 215 days of age although some vacuoles were seen in the cytoplasm from 110 days to 190 days of age.

A long-term surviving FALS patient with a frame-shift 126 mutation in the SOD1 gene

The clinical course and histopathological findings of this FALS patient with a clinical course of 11 years were reported previously by Kato et al. (1996). Severe neuronal loss with gliosis was recognized in the anterior

Fig. 2. A-C. Hematoxylin and eosin (HE) staining of liver sections of G1H-G93A transgenic mice in the pre-symptomatic stage of the first 90 days after birth **(A)**, at the onset of 100 days after birth **(B)** and at the end stage of 120 days after birth **(C)**. **D-F.** Immunohistochemical findings for peroxiredoxinI (PrxI) of liver sections of G1H-G93A mice in the presymptomatic stage of the first 90 days after birth **(D)**, at the onset of 100 days after birth **(E)** and at the end stage of 120 days after birth **(F)**. **A.** In the presymptomatic stage, two kinds of cells of swollen hydropic hepatocytes (arrows) and eosinophilic hepatocytes (arrowheads) are seen. The swollen hepatocytes have clear nuclei and a bright half-translucent cytoplasm that contain a few vacuoles about 5 μm in diameter. The eosinophilic hepatocytes have condensed nuclei and a dark eosinophilic cytoplasm with some vacuoles about 2 μm in diameter. The population of swollen hepatocytes is about 70% of total hepatocytes and the eosinophilic cells account for the remainder. The eosinophilic hepatocytes are scattered and intermingled among the swollen hepatocytes. **B.** At the onset stage, small sized-eosinophilic hepatocytes (arrowheads) represent about 80% of the cell population and the proportion of swollen hepatocytes (arrows) is correspondingly lower. Fewer vacuoles are present in the cytoplasm of the swollen hepatocytes. The vacuoles of the eosinophilic hepatocytes become smaller than those of the eosinophilic hepatocytes at 90 days of age. **C.** At the end stage, almost all of the hepatocytes are normal; neither swollen hydropic hepatocytes nor eosinophilic hepatocytes are observed. No vacuoles are observed in the hepatocytes. The histological findings in the liver at 120 days of age, corresponding to the end stage, are almost the same as those of the control G1H-G93A littermate mice. **D.** PrxI immunostaining of the hepatocytes in the pre-symptomatic stage. The PrxI-negative hepatocytes are intermingled with the positive hepatocytes in the pre-symptomatic stage. The normal zonal distributions of PrxI disappear in the pre-symptomatic stage. Approximately 80% of the swollen hepatocytes (arrows) and about 30% of the eosinophilic hepatocytes observed in HE preparations show immunoreactivity to PrxI. The other hepatocytes are negative for PrxI. Although most of the PrxI-expressing hepatocytes show the same staining intensity as that of control littermate hepatocytes, a few eosinophilic hepatocytes (arrowheads) strongly express PrxI. **E.** PrxI immunostaining of the hepatocytes at the onset. PrxI is overexpressed in both eosinophilic (arrowheads) and swollen hepatocytes (arrows). The staining intensity of the hepatocytes that are positive for PrxI is strongest at this stage. The normal zonal distribution of PrxI is not observed; a few negative hepatocytes are intermixed with the PrxI-positive hepatocytes. **F.** PrxI immunostaining of the hepatocytes at the end stage. Almost all of the hepatocytes show the same stainability and intensity as those of the hepatocytes of the normal littermates. Normal zonal distribution of PrxI is observed in this stage: hepatocytes in periportal areas stain more strongly for PrxI than those in the periterminal vein areas (asterisk). x 240

horn cells of the spinal cord, and neuronal LBHIs and astrocytic hyaline inclusions (Ast-His) were present (Kato et al., 1996, 1997). The liver showed neither fibrosis nor inflammation (Fig. 4A). Although no inclusion pathology such as neuronal LBHIs and Ast-His was evident in the hepatocytes, vacuolation pathology was obsereved in the hepatocytes (Fig. 4A).

Immunohistochemistry

Immunohistochemical findings in spinal cords of transgenic animals

When control and representative paraffin sections were incubated with PBS alone (i.e., no primary antibody), no staining was detected. The neuronal Lewy body-like hyaline inclusions (LBHIs) in ALS model animals with human mutant SOD1exhibited co-aggregation of PrxII/GPxI with SOD1. A breakdown of the redox system was observed in these motor neurons, which formed inclusions due to co-aggregation of PrxII/GPxI with SOD1. The Prxll/GPxl-immunoreactions in the four different phyletic lines of the ALS rat models (H46R and G93A rats) and ALS mouse models (G1H-G93A and G1L-G93A mice) were essentially the same throughout the disease course. In the preclinical stage, the Prxll/GPxl-immunostainability and immunointensity of the anterior horn cells were identical to those in normal anterior horn cells in the littermates. Although anterior horn cells in the ALS

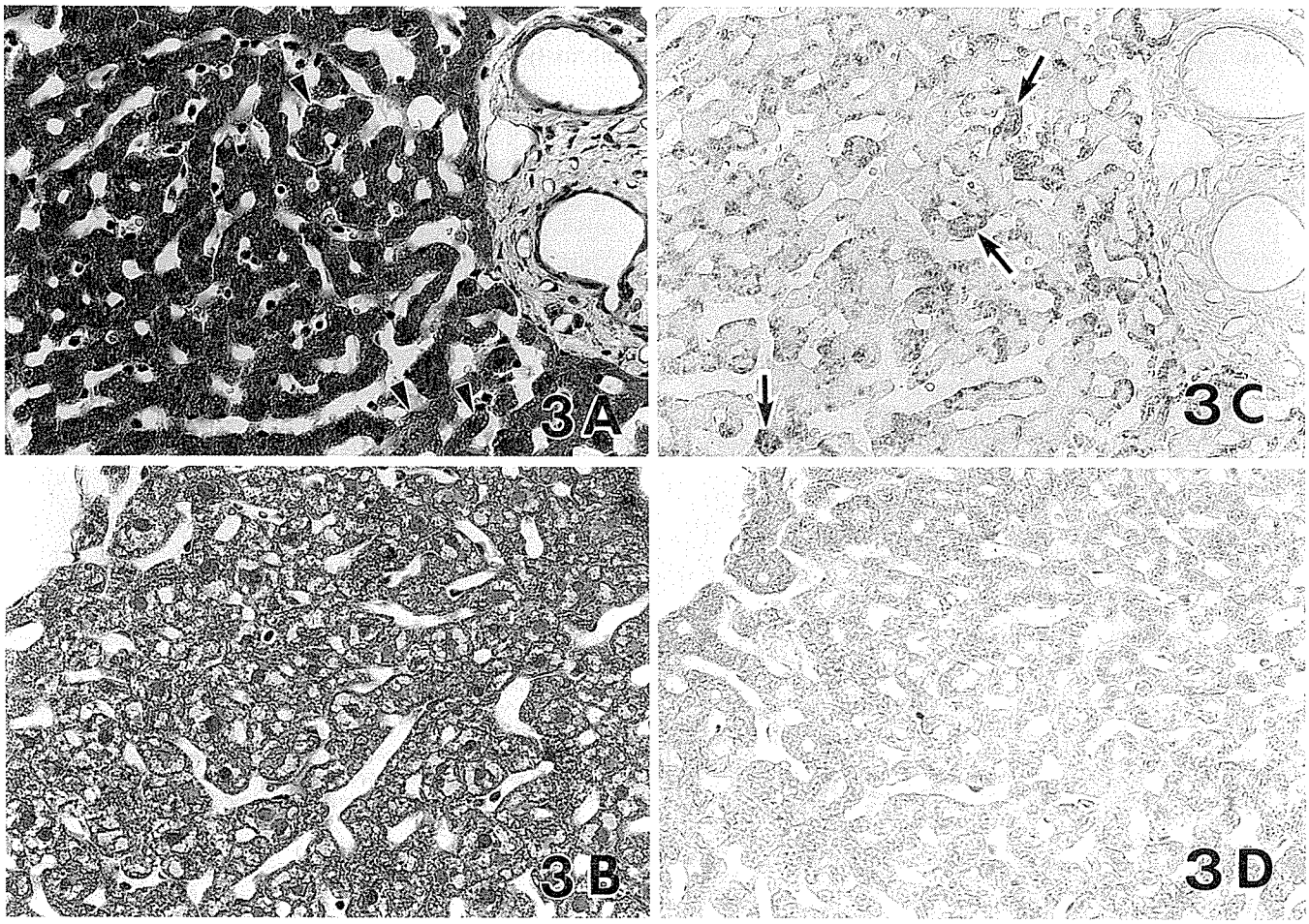

Fig. 3. A,B. Hematoxylin and eosin (HE) staining of the liver sections of G93A transgenic rats in the time of clinical onset at the age of 130 days after birth and of G1L-G93A transgenic mice in the presymtomatic stage at the age of 180 days after birth. **C, D.** Immunohistochemical staining of peroxiredoxinI (PrxI) in the liver sections of G93A transgenic rats in the time of clinical onset at the age of 130 days after birth and of G1H-G93A transgenic mice in the presymtomatic stage at the age of 180 days after birth. **A.** In G93A rats at 130 days of age, almost all of the hepatocytes appear histologically normal and are smaller than those of littermates. Some hepatocytes at 130 days of age contain about 1 μm in diameter (arrowheads). **B.** In G1L-G93A mice at 180 days of age, almost all of the hepatocytes are hydropic. In addition, several irregular intracytoplasmic slits containing some fluid-like material are seen. **C.** At 130 days of age in G93A rats, small hepatocytes that are predominant in HE preparations expressed PrxI intensely (arrows). **D.** At 180 days of age in G1L-G93A mice, the hepatocytes are immunostained intensely with the antibody against PrxI and the intracytoplasmic slits in hepatocytes are also strongly positive for PrxI. x 240

animal models were less abundant after clinical onset, some of these residual anterior horn cells overexpressed PrxII/GPxI, i.e., there was upregulation of the redox system. This upregulation in the residual motor neurons was most pronounced at 110 days of age in G1H-G93A mice, at 150 days in G93A rat, at 215 days in G1L-G93A mouse, and at 160 days in H46R rat. However, at the end stage in the four different strains of ALS model animals, almost all of the residual motor neurons showed no immunoreactivity for PrxII/GPxI, that is, they had undergone redox system breakdown, in marked contrast to the inclusions, which were positive for PrxII/GPxI.

Immunohistochemical findings in G1H-G93A transgenic mouse livers

In control littermate mice, PrxI, PrxII and GPxI (PrxI/PrxII/GPxI), which directly regulate the redox system, were expressed in the cytoplasm of almost all hepatocytes (Fig. 1B-D). The nuclei of some hepatocytes were also positive for PrxI and PrxII. Hepatocytes in the periportal areas stained more strongly for PrxI/PrxII/GPxI than those in the periterminal vein areas. Incubation of sections with the anti-rat PrxI or PrxII antibody that had been respectively pretreated with an excess amount of rat PrxI or PrxII produced no staining in any of the sections. The immunohistochemical results are summarized in Table 2. In contrast to the normal hepatocytes that were positive for the three proteins, the PrxI/PrxII/GPxI-negative hepatocytes were intermingled with the positive hepatocytes in the presymptomatic stage at 90 days after birth (Fig. 2D). Therefore, the normal zonal distribution of PrxI/PrxII/GPxI disappeared in the presymptomatic stage. Approximately 80% of the swollen hepatocytes and about 30% of the eosinophilic hepatocytes observed in HE preparations showed immunoreactivity to the redox-related proteins (Table 2). The other hepatocytes were negative for the three proteins. The staining intensity of PrxI/PrxII/GPxI was the same as that of

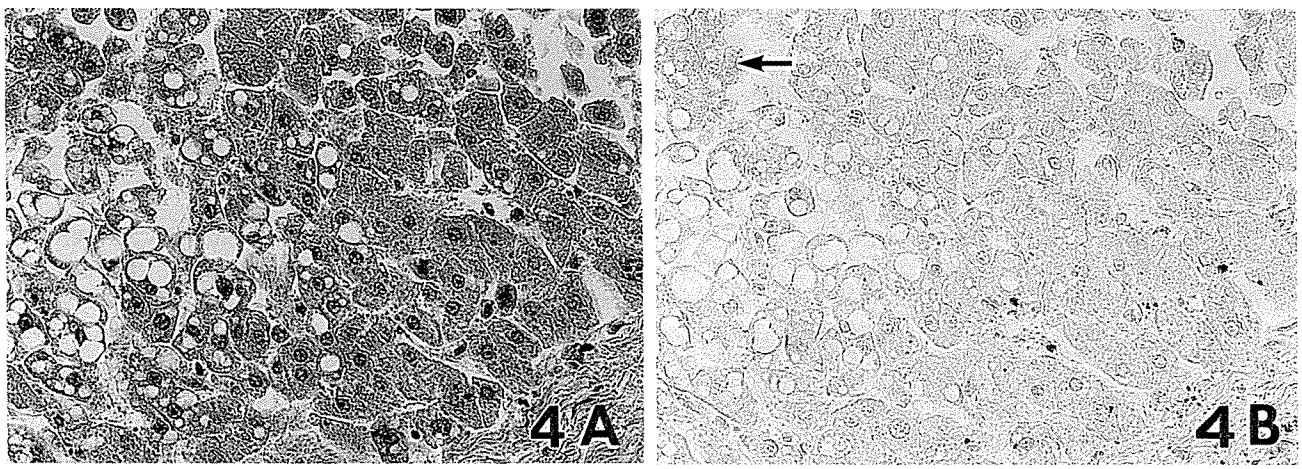

Fig 4. Hematoxylin and eosin staining **(A)** and immunohistohcemical staining of peroxiredoxinI (PrxI) **(B)** of the liver sections of the long-term surviving familial amyotrophic lateral sclerosis patient with a two-base-pair deletion at codon 126 in SOD1 gene. **A.** There are no fibrosis or inflammation in the liver. Although the inclusion pathology in the hepatocytes is not recognized, some vacuoles are observed in some hepatocytes. **B.** Most hepatocytes are faintly stained or unstained with the anti-PrxI antibody although a few hepatocytes weakly express PrxI (arrow). x 240

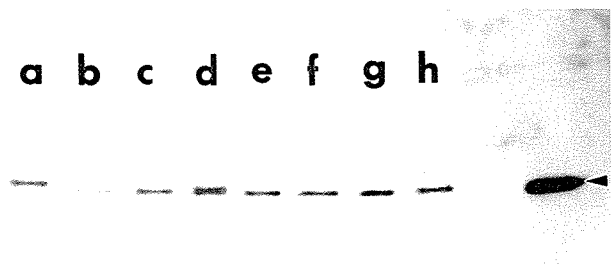

Fig. 5. Western blot analysis using the antibody against peroxiredoxinI (PrxI) of the liver. An exact 20-μg amount of the soluble protein extract from each sample was applied to each lane. Lane a: Control littermate mouse liver at 90 days after birth, lane b: G1H-G93A transgenic mouse liver at 90 days after birth, lane c: control littermate mouse liver at 100 days after birth, lane d: G1H-G93A transgenic mouse liver at 100 days after birth, lane e: control littermate mouse liver at 110 days after birth, lane f: G1H-G93A transgenic mouse liver at 110 days after birth, lane g: control littermate mouse liver at 120 days after birth, lane h: G1H-G93A transgenic mouse liver at 120 days after birth. A single band at the position corresponding to PrxI (a molecular mass approximately 23 kDa) (arrowhead) is observed in transgenic mice and control littermate mice. The intensity of PrxI immunoreactivity in the G1H-G93A mice at 90 days of age is slightly less than those in the G1H–G93A mice at 110 and 120 days of age whose PrxI immunoreactivity appears to be almost identical to that in the littermate mice. The intensity of PrxI immunoreactivity in the G1H-G93A mice at 100 days of age is slightly stronger than those in the G1H–G93A mice at 110 and 120 days of age. This observation supports the results of PrxI immunohistochemistry.

control littermate hepatocytes. Most hepatocytes expressed these three proteins synchronously. However, certain hepatocytes that were positive for PrxI/PrxII were negative for GPxI, and some hepatocytes negative for PrxI/PrxII were positive for GPxI. At 100 days of age, the normal zonal distribution of PrxI/PrxII/GPxI was not observed; the PrxI/PrxII/GPxI-negative hepatocytes were intermixed with the positive hepatocytes (Fig. 2E). Approximately 75% of the swollen hepatocytes and about 80% of eosinophilic hepatocytes were positive for PrxI/PrxII/GPxI (Table 2). The staining intensity of the hepatocytes that were positive for the three redox-related proteins was strongest at this stage. After the onset and until the end stage, i.e., during the motor deficit stage, almost all of the hepatocytes showed normal stainability with normal intensity: the stainability and intensity in the hepatocytes of the motor deficit stage were identical to those in the littermates' hepatocytes (Fig. 2F). Furthermore, the normal zonal distribution of PrxI/PrxII/GPxI was observed during the motor deficit stage. The expression of PrxI/PrxII/GPxI in the intersinusoidal cells was similar to that of hepatocytes throughout the disease course. Although all intersinusidal cells expressed these three proteins in the liver of G1H-G93A littermates, some intersinusoidal cells were negative in the presymptpmatic stage. Finally, the three redox-related proteins were expressed in the intersinusoidal cells at the end stage.

Immunohistochemical findings in G93A and H46R transgenic rat livers

In control littermate rats, almost all of the hepatocytes expressed PrxI/PrxII/GPxI identically to those in the littermate mouse livers. At 70 and 90 days of age in G93A rats, PrxI/PrxII/GPxI was expressed in the cytoplasm of the hepatoctyes and the zonal distribution was normal. In the presymptomatic stage at 110 days of age in G93A rats, many of both the swollen and eosinophilic hepatocytes were positive for these redox-related proteins, with normal intensity. However, some negative hepatocytes were intermingled with positive hepatocytes. At 130 days of age in G93A rats, small hepatocytes that were predominant in HE preparations expressed these redox-related proteins intensely: the staining intensity was strongest at this stage throughout the disease course (Fig. 3C). At the end stage in G93A and H46R rats, almost all of the hepatocytes showed the same stainability and intensity as those of the hepatocytes of the normal littermates.

Immunohistochemical findings in G1L-G93A transgenic mice liver

In the preclinical stage at 110,120 and 150 days of age, almost all of the normal hepatocytes in HE preparations expressed Prxl/Prxll/GPxl. At 150 days of age, some of the hydropic hepatocytes were moderately positive for Prxl/Prxll/GPxl and other swelling hepatocytes were negative; the negative hepatocytes were intermixed with positive cells. The vacuoles in the cytoplasm of the hepatocytes were almost negative for Prxl/Prxll/GPxl. Prxl/Prxll/GPxl was expressed in some intersinusoidal cells. At 180 and 190 days of age, the hepatocytes were immunostained intensely with the three antibodies against Prxl/Prxll/GPxl and the intracytoplasmic slits in hepatocytes that contained some fluid were also strongly positive for Prxl/Prxll/GPxl (Fig. 3D). At 215 days of age, almost all of the hepatocytes expressed Prxl/Prxll/GPxl. At the end stage, beyond 250 days of age, the stainability and intensity in many hepatocytes were lower than in the hepatocytes in the control littermates, although some hepatocytes showed the same stainability and intensity of Prxl/Prxll/GPxl as those in the control littermates. The intersinusoidal cells showed similar staining patterns to those of hepatocytes.

Immunohistochemical findings in the liver and spinal cord of a long-term surviving FALS patient with a frame-shift 126 mutation in the SOD1 gene

As expected, some neuronal inclusions were positive for PrxII and GPxI in this long-surviving patient. The cytoplasm of the other remaining motor neurons did not express PrxII/GPxI. In the liver, most hepatocytes are faintly stained or unstained with the antibodies against

Table 2. Immunohistochemical results of PrxI/PrxII/GPxI expression in the hepatocytes of G1H-G93A mice .

Days after birth	90 days		100 days		110 days	120 days
Cell type in HE staining	Swollen hepatocytes	Eosinophilic hepatocytes	Swollen hepatocytes	Eosinophilic hepatocytes	Normal hepatocytes	Normal hepatocytes
A ratio of PrxI-positive each-type hepatocytes to each type hepatocytes (PrxI+/each-type total cells)	76.1±2.1%*	32.3±2.0%	78.5±2.5%	40.2±1.8%	100%	100%
PrxII+/each-type total cells	73.8±1.6%	31.4±1.1%	75.5±1.7%	42.0±1.7%	100%	100%
GPxI+/each type total cells	77.0±1.2%	35.1±1.6%	81.1±2.3%	42.1±1.4%	100%	100%

*The number present mean ± standard error.

PrxI/PrxII/GPxI although a few hepatocytes weakly express PrxI (Fig. 4B) /PrxII/GPxI.

Western blot analyses

When homogenates of fresh liver of the G1H–G93A mice were examined by immunoblotting for Prxl, a single band at the position corresponding to a molecular mass of approximately 23 kDa was observed (Fig. 5). Immunoblotting showed that the intensity of Prxl immunoreactivity in the G1H-G93A mice at 90 days of age is slightly less than those in the G1H-G93A mice at 110 and 120 days of age whose Prxl immunoreactivity appears to be almost identical to that in the littermate mice. The intensity of Prxl immunoreactivity in the G1H-G93A mice at 100 days of age is slightly stronger than those in the G1H-G93A mice at 110 and 120 days of age. This observation supported the results of Prxl immunohistochemistry.

Discussion

Although the neuropathology of the motor neurons in ALS including the SALS patients of unknown etiology, mutant SOD1-linked FALS and ALS model animals expressing human mutant SOD1 genes has been investigated in detail (Dal Canto and Gurney, 1995; Wong et al., 1995; Hirano, 1996; Kato et al., 1999), the pathology of the liver has been neglected because failure of liver function is not a feature of ALS. In the present study, for the first time, significant histopathological findings in common were found in both motor neurons and hepatocytes in the four different strains of mutant SOD1-linked ALS model animals. Furthermore, the hepatic histopathological findings changed dramatically during the course of the diseases. The common histopathological findings in the livers in the mutant SOD1-linked ALS model animals were hydropic swelling and eosinophilic changes with vacuolation pathology. Notably, these histopathological changes in the hepatocytes disappeared at the end stage and almost all of the hepatocytes appeared to be normal, not only in HE preparations but also in redox system-related immunohistochemical preparations. Previous histopathological liver findings among SALS patients of unknown etiology included, ultrastructural analyses of liver biopsy findings of 21 ALS patients that showed bizarre mitochondria, intramitochondrial paracrystalline inclusions, disorganization of the lamellar structure of the rough endoplasmic reticulum, more abundant smooth endoplasmic reticulum and parasinusoidal fibrosis (Nakano et al., 1987), but the relationship between these hepatic findings and ALS pathogenesis remains unclear. The present paper is the first to demonstrate significant histopathological findings in hepatocytes during the course of the disease in ALS model animals with a SOD1 mutation as the known etiology.

The common histopathological findings in the livers of the four different phyletic lines of the ALS rat models (H46R and G93A rats) and ALS mouse models (G1H-G93A and G1L-G93A mice) were hydropic swelling and eosinophilic changes with vacuole formation though there were some differences in the copy number of the transgene. The first prominent histopathological finding in the livers of G1H-G93A mice was hydropic degeneration or ballooned swelling of hepatocytes before and around the onset of neurological symptoms. The second striking finding was cytoplasmic eosinophilic degeneration with nuclear condensation of hepatocytes around the time of onset. These two main findings were similar to ballooning or atrophic changes in hepatocytes in acute intoxication after administration of chemical substances such as carbon tetrachloride (Yeldandi et al., 1996). These histopathological findings seem to coincide with hepatic degeneration in drug-induced hepatic injury (Yeldandi et al., 1996). Therefore, it was suggested that the histopathological features of the G1H-G93A liver reflect a type of intoxication by human mutant SOD1 protein that originates from the human SOD1 gene with the G93A mutation.

Vacuolation pathology and motor neuron death with inclusion pathology in the spinal cord are the essential neuropathological findings in ALS model animals (Dal Canto and Gurney, 1995; Wong et al., 1995; Kato et al., 1999). The vacuolation pathology was found before onset of the neurological symptoms (Dal Canto and Gurney, 1995; Wong et al., 1995). Similar vacuole formation was found in the hepatocytes before the onset of neurological symptoms, as it was in motor neurons. From the fact that the vacuolation pathology was observed in both motor neurons and hepatocytes at almost the same disease stage, the common ALS stress of mutant SOD1 is considered to cause histopathological changes of the liver and the spinal cord of ALS model animals in the early stage of the disease. The comparison between hepatocytes and motor neurons is meaningful from the viewpoint of generalized mutant SOD1 disease. Although the hepatocytes and motor neurons in the ALS model animals were under the same ALS stress in the early stages, the histopathological features of the hepatocytes were different from those in motor neurons at the end stage. In other words, the number of motor neurons fell gradually and the inclusion pathology appeared toward the end stage; however, cell death with inclusion pathology was not found in the hepatocytes. We showed that there was a difference in immunohistochemical expression of the redox system related proteins PrxI, PrxII and GPxI to explain this discrepancy between hepatocytes and motor neurons.

The zonal localization of PrxI and GPxI-expressing hepatocytes in the hepatic lobules of the control livers was consistent with previous reports (Sunde and Hoekstra, 1980; Immenschuh, 2003), and this immunohistochemical finding implies that the liver contains abundant redox system-related enzymes. In association with the histopathological changes in the livers from the presymptomatic stages to the onset of neurological symptoms in G1H-G93A mice, the zonal

distribution of redox system-related enzymes in the livers was immunohistochemically absent, and the hepatocytes expressing the redox-related enzymes and those not expressing these enzymes were intermingled in various ratios. The hepatocytes that overexpressed the redox system-related enzymes were evident among the hepatocytes expressing these enzymes. In addition to these immunohistochemical data, Western blot results also supported the observation that the redox system-related enzymes were overinduced in some hepatocytes. Overinduction of redox system-related enzymes in the hepatocytes was observed around the time of clinical onset. By marked contrast, the SOD1-mutated motor neurons that formed inclusions showed intra-inclusional co-aggregation of redox proteins with SOD1, thereby reducing the availability of the redox system (Kato et al., 2004). Among motor neurons without inclusions, some exposed to mutant SOD1 stress (i.e., ALS stress) are capable of overexpressing redox system-related enzymes as one of their vital physiological reactions, although many SOD1-mutated motor neurons showed disruption of the redox system (Kato et al., 2005). Neurons under long-term ALS stress no longer have the ability to upregulate the redox system, and as ALS progresses, these residual ALS neurons finally become unable even to maintain the redox system itself (Kato et al., 2005). Therefore, unlike the situation in hepatocytes, breakdown of the redox system in SOD1-mutated motor neurons results in cell death. The redox system-related enzymes that are abundant in the liver (Immenschuh et al., 2003) convert superoxide radicals into hydrogen peroxide that is immediately converted by SOD1 to harmless water and oxygen. Because SOD1 is rich in the liver under physiological conditions (Marklund, 1980), mutant SOD1 is also induced abundantly in the liver of ALS model animals with the SOD1 gene mutation. Although hepatocytes in G1H-G93A mice are exposed to mutant SOD1 stress throughout life, in order to protect themselves from the mutant SOD1 stress, these hepatocytes are able to keep on inducing the redox system-related enzymes and maintaining the redox system. However, it is considered impossible for hepatocytes under long-term mutant SOD1 stress to keep on inducing these redox system-related enzymes. Therefore, hepatocytes under long-term mutant SOD1 stress, e.g., the hepatocytes in the FALS patient with the 11-year disease course and in the end-stage G1L-G93A mice, eventually become unable to maintain the redox system. On the other hand, there are many reports that diverse stresses dangerous to cell survival result in the overinduction of redox system-related enzymes, contributing to the regulation of signal transduction (Andoh et al., 2003; Biteau et al., 2003; Georgiou, 2003; Neuman et al., 2003; Wood et al., 2003; Chang et al., 2004). This redox signal transduction is linked to important systems such as cellular differentiation, immune response, growth control, apoptosis, and tumor growth (Jin et al., 1997; Berggren et al., 2001; Koo et al., 2002; Chang et al., 2002; Mu et al., 2002; Neuman et al., 2003). Redox system-related enzymes are overinduced in reaponse to survival-threatening stresses such as mutant SOD1. Our findings suggest that the up-regulation of redox system-related enzymes may rescue cells from death under mutant SOD1 stress. Therefore, we postulate that our data will lead to the development of a new therapy based on redox system up-regulation for the treatment of ALS, which for over 130 years has had an unknown etiology.

Acknowledgments. This study was supported in part by a Grant-in-Aid for Scientific Research (c) (S.K.: 17500229) and a Grant-in-Aid for Scientific Research in Priority Area (T.N.) from the Ministry of Education, Culture, Sports, Science and Technology of Japan, by a Research Grant on Measures for Intractable Diseases from the Ministry of Health, Labour and Welfare of Japan (S.K. and Y.I.), and by a Grant from Research on Psychiatric and Neurological Disease and Mental Health (S.K., M.A. and Y.I.)

References

Abe Y. and Okazaki T. (1987). Purification and properties of the manganese superoxide dismutase from the liver of bullfrog, Rana catesbeiana. Arch. Biochem. Biophys. 253, 241-248.

Andoh T., Chiueh C.C. and Chock P.B. (2003). Cyclic GMP-dependent protein kinase regulates the expression of thioredoxin and thioredoxin peroxidase-1 during hormesis in response to oxidative stress-induced apoptosis. J. Biol. Chem. 278, 885-890.

Berggren M.I., Husbeck B., Samulitis B., Baker A.F., Gallegos A. and Powis G. (2001). Thioredoxin peroxidase-1 (peroxiredoxin-1) is increased in thioredoxin-1 transfected cells and results in enhanced protection against apoptosis caused by hydrogen peroxide but not by other agents including dexamethasone, etoposide, and doxorubicin. Arch. Biochem. Biophys. 392,103-109.

Biteau B., Labarre J. and Toledano M.B. (2003). ATP-dependent reduction of cysteine-sulphinic acid by S. cerevisiae sulphiredoxin. Nature 425, 980-984.

Chae H.Z., Kim I.H., Kim K. and Rhee S.G. (1993). Cloning, sequencing, and mutation of thiol-specific antioxidant gene of Saccharomyces cerevisiae. J. Biol. Chem. 268, 16815-16821.

Chae H.Z., Robison K., Poole L.B., Church G., Storz G. and Rhee S.G. (1994). Cloning and sequencing of thiol-specific antioxidant from mammalian brain: alkyl hydroperoxide reductase and thiol-specific antioxidant define a large family of antioxidant enzymes. Proc. Natl. Acad. Sci. USA 91, 7017-7021.

Chang T.S., Jeong W., Choi S.Y., Yu S., Kang S.W. and Rhee S.G. (2002). Regulation of peroxiredoxin I activity by cdc2-mediated phosphorylation. J. Biol. Chem. 277, 25370-25376.

Chang T.S., Jeong W., Woo H.A., Lee S.M., Park S. and Rhee S.G. (2004). Characterization of mammalian sulfiredoxin and its reactivation of hyperoxidized peroxiredoxin through reduction of cysteine sulfinic acid in the active site to cysteine. J. Biol. Chem. 279, 50994-51001.

Charcot J.M. and Joffroy A. (1869). Deux cas d'atrophie musculaire progressive avec lésions de la substance grise et des faisceaux antéro-latéraux de la moelle épinière. Arch. Physiol. (Paris) 2, 744-760.

Dal Canto M.C. and Gurney M.E. (1995). Neuropathological changes in

two lines of mice carrying a transgene for mutant human Cu,Zn SOD, and in mice overexpressing wild type human SOD: a model of familial amyotrophic lateral sclerosis (FALS). Brain Res. 676, 25-40.

de Belleroche J., Orrell R.W. and Virgo L. (1996). Amyotrophic lateral sclerosis: recent advances in understanding disease mechanisms. J. Neuropathol. Exp. Neurol. 55, 747-757.

de Haan J.B., Bladier C., Griffiths P., Kelner M., O'Shea R.D., Cheung N.S., Bronson R.T., Silvestro M.J., Wild S., Zheng S.S., Beart P.M., Hertzog P.J. and Kola I. (1998). Mice with a homozygous null mutation for the most abundant glutathione peroxidase, Gpx1, show increased susceptibility to the oxidative stress-inducing agents paraquat and hydrogen peroxide. J. Biol. Chem. 273, 22528-22536.

Deng H.X., Hentati A., Tainer J.A., Iqbal Z., Cayabyab A., Hung W.Y., Getzoff E.D., Hu P., Herzfeldt B., Roos R.P., Warner C., Deng G., Soriano E., Smyth C., Parge H.E. Ahmed A., Roses A.D., Hallewell R.A., Pericak-Vance M.A and Siddique T. (1993). Amyotrophic lateral sclerosis and structural defects in Cu,Zn superoxide dismutase. Science 261, 1047-1051.

Fridovich I. (1986). Superoxide dismutases. Adv. Enzymol. Relat. Area Mol. Biol. 58, 61-97.

Georgiou G. and Masip L. (2003). An overoxidation journey with a return ticket. Science 300, 592-594.

Gurney M.E., Pu H., Chiu A.Y., Dal Canto M.C., Plochow C.W., Alexander D.D., Caliendo J., Hentati A., Kwon Y.W., Deng H.X., Chen W., Zhai P., Sufit R.L. and Siddique T. (1994). Motor neuron degeneration in mice that express a human Cu,Zn superoxide dismutase mutation. Science 264, 1772-1775.

Hirano A. (1996). Neuropathology of ALS: an overview. Neurology 47, S63-66.

Hirotsu S., Abe Y., Nagahara N., Hori H., Nishino T., Okada K. and Hakoshima T. (1999a). Crystallographic characterization of a stress-induced multifunctional protein, rat HBP-23. J. Struct. Biol. 126, 80-83.

Hirotsu S., Abe Y., Okada K., Nagahara N., Hori H., Nishino T. and Hakoshima T. (1999b). Crystal structure of a multifunctional 2-Cys peroxiredoxin heme-binding protein 23 kDa/proliferation-associated gene product. Proc. Natl. Acad. Sci. USA 96,12333-12338.

Hofmann B., Hecht H.J. and Flohe H. (2002). Peroxiredoxins. Biol. Chem. 383, 347-364.

Hudson A.J. (1981). Amyotrophic lateral sclerosis and its association with dementia, parkinsonism and other neurological disorders: a review. Brain 104, 217-247.

Immenschuh S., Baumgart-Vogt E., Tan M., Iwahara S., Ramadori G. and Fahimi H.D. (2003). Differential cellular and subcellular localization of heme-binding protein 23/peroxiredoxin I and heme oxygenase-1 rat liver. J. Histochem. Cytochem. 51, 1621-1631.

Iwahara S., Satoh H., Song D.X., Webb J., Burlingame A.L., Nagae Y. and Muller-Eberhard U. (1995). Purification, characterization, and cloning of a heme-binding protein (23 kDa) in rat liver cytosol. Biochemistry 34, 13398-13406.

Jin D.Y., Chae H.Z., Rhee S.G. and Jeang K.T. (1997). Regulatory role for a novel human thioredoxin peroxidase in NF-kappaB activation. J. Biol. Chem. 272, 30952-30961.

Juneja T., Pericak-Vance M.A., Laing N.G., Dave S. and Siddique T. (1997). Prognosis in familial amyotrophic lateral sclerosis: progression and survival in patients with glu100gly and ala4val mutations in Cu,Zn superoxide dismutase. Neurology 48, 55-57.

Kato S., Shimoda M., Watanabe Y., Nakashima K., Takahashi K. and Ohama E. (1996). Familial amyotrophic lateral sclerosis with a two base pair deletion in superoxide dismutase 1 gene: multisystem degeneration with intracytoplasmic hyaline inclusions in astrocytes. J. Neuropathol. Exp. Neurol. 55,1089-1101.

Kato S., Hayashi H., Nakashima K., Nanba E., Kato M., Hirano A., Nakano I., Asayama K. and Ohama E. (1997). Pathological characterization of astrocytic hyaline inclusions in familial amyotrophic lateral sclerosis. Am. J. Pathol. 151, 611-620.

Kato S., Saito M., Hirano A. and Ohama E. (1999). Recent advances in research on neuropathological aspects of familial amyotrophic lateral sclerosis with superoxide dismutase 1 gene mutations: neuronal Lewy body-like hyaline inclusions and astrocytic hyaline inclusions. Histol. Histopathol. 14, 973-989.

Kato S., Takikawa M., Nakashima K., Hirano A., Cleveland D.W., Kusaka H., Shibata N., Kato M., Nakano I. and Ohama E. (2000). New consensus research on neuropathological aspects of familial amyotrophic lateral sclerosis with superoxide dismutase 1 (SOD1) gene mutations: Inclusions containing SOD1 in neurons and astrocytes. ALS Other Motor Neuron Disorders 1, 163-184.

Kato S., Shaw P., Wood-Allum C., Leigh P.N. and Show C. (2003). Amyotrophic lateral sclerosis, In: Nerodegeneration: The molecular pathology of dementia and movement disorders. Dickson D. (ed) ISN Neuropath Press, Basel. pp 350-368.

Kato S., Saeki Y., Aoki M., Nagai M., Ishigaki A., Itoyama Y., Kato M., Asayama K., Awaya A., Hirano A. and Ohama E. (2004). Histological evidence of redox system breakdown caused by superoxide dismutase 1 (SOD1) aggregation is common to SOD1-mutated motor neurons in humans and animal models. Acta Neuropathol. 107, 149-158.

Kato S., Kato M., Abe Y., Matsumura T., Nishino T., Aoki M., Itoyama Y., Asayama K., Awaya A., Hirano A and Ohama E. (2005). Redox system expression in the motor neurons in amyotrophic lateral sclerosis (ALS): immunohistochemical studies on sporadic ALS, superoxide dismutase 1 (SOD1)-mutated familial ALS, and SOD1-mutated ALS animal models. Acta Neuropathol. 110, 101-112.

Koo K.H., Lee S., Jeong S.Y., Kim E.T., Kim H.J., Kim K., Song K. and Chae H.Z. (2002). Regulation of thioredoxin peroxidase activity by c-terminal truncation. Arch. Biochem. Biophys. 397, 312-318.

Marklund S. (1980). Distribution of CuZn superoxide dismutase and Mn superoxide dismutase in human tissues and extracellular fluids. Acta Physiol. Scand. Suppl. 492,19-23.

Matsumoto A., Okado A., Fujii T., Fujii J., Egashira M., Niikawa N. and Taniguchi N. (1999). Cloning of the peroxiredoxin gene family in rats and characterization of the fourth member. FEBS Lett. 443, 246-250.

Mu Z.M., Yin X.Y. and Prochownik E.V. (2002). Pag, a putative tumor suppressor, interacts with the myc box II domain of c-myc and selectively alters its biological function and target gene expression. J. Biol. Chem. 277, 43175-43184.

Nagai M., Aoki M., Miyoshi I., Kato M., Pasinelli P., Kasai N., Brown Jr R.H. and Itoyama Y. (2001). Rats expressing human cytosolic copper-zinc superoxide dismutase transgenes with amyotrophic lateral sclerosis: associated mutations develop motor neuron disease. J. Neurosci. 21, 9246-9254.

Nakano Y., Hirayama K. and Terao K. (1987). Hepatic ultrastructural changes and liver dysfunction in amyotrophic lateral sclerosis. Arch. Neurol. 44, 103-106.

Neumann C.A., Krause D.S., Carman C.V., Das S., Dubey D.P., Abraham J.L., Bronson R.T., Fujiwara Y., Orkin S.H. and Van Etten R.A. (2003). Essential role for the peroxiredoxin prdx1 in erythrocyte

antioxidant defence and tumour suppression. Nature 424, 561-565.

Prosperi M.T, Ferbus D., Karczinski I. and Goubin G. (1993). A human cDNA corresponding to a gene overexpressed during cell proliferation encodes a product sharing homology with amoebic and bacterial proteins. J. Biol. Chem. 268, 11050-11056.

Rosen D.R., Siddique T., Patterson D., Figlewicz D.A., Sapp P., Hentati A., Donaldson D., Goto J., O'Regan J.P., Deng H.-X., Rahmani Z., Krizus A., McKenna-Yasek D., Cayabyab A., Gaston S.M., Berger R., Tanzi R.E., Halperin J.J., Herzfeldt B., Van den Bergh R., Hung W.-Y., Bird T., Deng G., Mulder D.W., Smyth C., Laing N.G., Soriano E., Pericak-Vance M.A., Haines J., Rouleau G.A., Gusella J.S., Horvitz H.R. and Brown R.H.Jr. (1993). Mutations in Cu/Zn superoxide dismutase gene are associated with familial amyotrophic lateral sclerosis. Nature 362, 59-62.

Sen C.K. and Packer L. (1996). Antioxidant and redox regulation of gene transcription. FASEB J. 10, 709-720.

Siddique T., Figlewicz D.A., Pericak-Vance M.A., Haines J.L., Rouleau G., Jeffers A.J., Sapp P., Hung W.Y., Bebout J., McKenna-Yasek D., Deng G., Horvitz H,R., Gusella J.F., Brown R.H.Jr and Roses A.D. (1991). Linkage of a gene causing familial amyotrophic lateral sclerosis to chromosome 21 and evidence of genetic-locus heterogeneity. N. Engl. J. Med. 324, 1381-1384.

Sunde P.A. and Hoekstra W.G. (1980). Structure, synthesis and function of glutathione peroxidase. Nutr. Rev. 38, 265-273.

Wen S.-T. and Van etten R.A. (1997). The PAG gene product, a stress-induced protein with antioxidant properties, is an Abl SH3-binding protein and a physiological inhibitor of c-Abl tyrosine kinase activity. Gene Dev. 11, 2456-2467.

Westman N.G. and Marklund S.L. (1981). Copper- and zinc-containing superoxide dismutase and manganese-containing superoxide dismutase in human tissues and human malignant tumors. Cancer Res. 41, 2962-2966.

Wong P.C., Pardo C.A., Borchelt D.R., Lee M.K., Copeland N.G., Jenkins N.A., Sisodia S.S., Cleveland D.W. and Price D.L. (1995). An adverse property of a familial ALS-linked SOD1 mutation causes motor neuron disease characterized by vacuolar degeneration of mitochondria. Neuron 14,1105-1116.

Wood Z.A., Poole L.B. and Karplus P.A. (2003). Peroxiredoxin evolution and the regulation of hydrogen peroxide signaling. Science 300, 650-653.

Yeldandi A.V., Kaufman D.G. and Reddy J.K. (1996). Cell injury and cellular adaptations. In: Anderson's Pathology. 10th ed. Damjanov I. and Linder J. (eds). Mosby. St. Louis. pp 357-386.

Accepted February 3, 2006